

Metal oxides as combustion catalysts for a stratified, dual bed partial oxidation catalyst

B.N.T. Nguyen, C.A. Leclerc*

Department of Chemical Engineering, McGill University, 3610 University St., Montréal, Qué., Canada H3A 2B2

Received 12 January 2006; received in revised form 10 February 2006; accepted 13 February 2006

Available online 31 March 2006

Abstract

Bimetallic, dual bed catalysts made up of metal oxides were investigated in the millisecond catalytic partial oxidation of methane to synthesis gas. A metal oxide combustion catalyst containing manganese, chromium, or copper was coupled with a nickel reforming catalyst to carry out the partial oxidation of methane. These catalysts produce hydrogen yields that compare to a platinum/nickel dual bed catalyst at a fraction of the cost. The high space velocity of the millisecond reactor improves performance by giving high rates of heat convection from the exothermic, upstream combustion catalyst to the downstream, endothermic reforming catalyst. Additionally, over a 10 h experiment, the catalyst activity did not decrease.

© 2006 Elsevier B.V. All rights reserved.

Keywords: Hydrogen; Partial oxidation; Syngas; Metal oxide; Fuel processing; Millisecond reactor

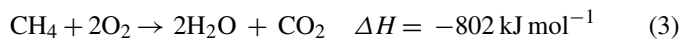
1. Introduction

For on-board processing of fuel to hydrogen, the catalytic partial oxidation process (1) has several advantages over steam reforming (2).



The major benefits of partial oxidation over steam reforming are a 2–3 order of magnitude decrease in residence time [1,2], faster start-up [3,4] and the ability to easily reform a wide array of fuels, including methane [5,6], alcohols [7–9], gasoline [10] and diesel [11,12]. These traits lead to a partial oxidation reformer that uses a catalyst support on the order of inches in diameter and an inch thick that is capable of reforming a wide variety of fuels to hydrogen for an automobile in under 5 s. One major drawback of partial oxidation is that rhodium is the most stable and active metal to catalyze this reaction [13]. In comparison, steam reforming uses nickel, which is orders of magnitude cheaper than rhodium.

Recently, it has been reported that stratified beds of platinum and nickel obtain comparable activity and stability to rhodium for catalytic partial oxidation of methane at about half the cost [14]. This catalyst works on the basis that partial oxidation (1) can be divided into combustion (3) and a pair of reforming reactions, steam (2) and dry (4) reforming.



The previous work used platinum for combustion and nickel for reforming. In this work, the stratified bed concept is extended to make use of metal oxides as combustion catalysts. In reviews of catalytic combustion, cobalt, manganese, copper and chromium have been identified as active metal oxide combustion catalysts [15,16]. In this work, cobalt was not examined, since it has been shown previously that cobalt deactivates rapidly at this feed rate and stoichiometry [13].

There are a number of contributions in the literature that investigate the use of metal oxides in the catalytic combustion of methane. However, most of these investigations look at the combustion of methane in excess oxygen diluted with either helium or nitrogen. Zaki et al. [17] investigated the oxidation of methane on manganese oxide supported on various ceramics. Using feeds of methane and excess oxygen diluted in helium,

* Corresponding author. Tel.: +1 514 398 8308; fax: +1 514 398 6678.
E-mail address: corey.leclerc@mcgill.ca (C.A. Leclerc).

they found that silica-alumina was the best support and that the catalyst was chemically and structurally stable. Wang and Xie [18,19] tested doped manganese oxide catalysts for deep oxidation of methane and excess oxygen diluted in nitrogen and found comparable activity to palladium especially at low temperatures (<420 °C). Marion et al. [20] tested the activity of copper oxide loaded on alumina for methane combustion with excess oxygen diluted in nitrogen. They found high activity and stable operation in an aging study conducted at temperatures less than 1000 °C. Artizzu et al. [21] found that by using a spinel support for the copper oxide, the catalyst would not degrade at 1000 °C. Anderson et al. [22] tested a number of metals for the catalysis of methane combustion in excess oxygen without a diluent. They found that, besides noble metals, chromium oxide supported on alumina was the most active catalyst for methane combustion. No information was found for the catalytic combustion of methane under fuel rich conditions at high space velocities for any of the metal oxides based on copper, chromium or manganese.

The major benefit of using a metal oxide catalyst is the price. In the platinum/nickel dual bed catalyst, the major cost is the platinum. The platinum/nickel catalyst is much cheaper than rhodium, but it is still expensive. The average price of platinum in 2004 was US\$ 27,400 kg⁻¹ [23]. The metals used to produce the metal oxides are much cheaper than platinum. According to the US Geological Survey, copper was US\$ 2.91 kg⁻¹ and chromium was US\$ 5.38 kg⁻¹ in 2004. The price for pure manganese was not available, though the price is not expected to be orders of magnitude higher than chromium or copper. Eliminating platinum from the dual bed catalyst will greatly reduce the price of the catalyst, since nickel was only US\$ 13.83 kg⁻¹.

In this work, dual bed partial oxidation catalysts utilizing manganese, copper and chromium oxides for combustion and nickel for reforming were compared to previous results for a platinum combustion catalyst followed by a nickel reforming catalyst. In all cases, the relative space velocity for the combustion catalyst and the reforming catalyst were equal. In this work, dual bed catalysts are denoted only by the metal used in the combustion section, even though the metal oxide is used as a catalyst. The effects of methane to oxygen (C/O) ratio in the feed and the gas hourly space velocity (GHSV) were examined. Catalyst degradation studies were performed by observing the reactant conversions, product selectivities and back face temperature over 10 h on stream.

2. Experimental

2.1. Apparatus

A schematic of the reactor is shown in Fig. 1. The reactor consisted of a quartz tube of 18 mm in inner diameter. The catalytic metal is supported on an 80 pores per inch (ppi) foam monolith composed of α -alumina. The catalytic foam monolith was placed in between two blank, 45 ppi monoliths, which acted as axial heat shields. The monoliths are wrapped in Fiberglass, an alumino-silicate paper, to prevent gas bypass. A K-type thermocouple is placed through the downstream heat shield to

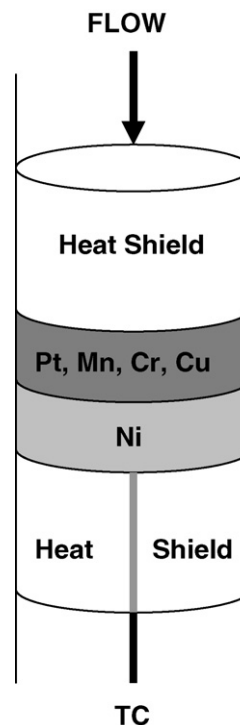


Fig. 1. A schematic of the sequential bed catalyst. The sequential bed catalyst is made up of two 5 mm monoliths. In this work, the first monolith is coated with metal oxides of manganese, copper or chromium. The second monolith was coated with nickel.

make contact with the back face of the second catalytic (nickel oxide) monolith. The temperatures reported in Section 3 are the back face temperatures. Gases are fed thru Tylan mass flow controllers.

The catalyst is lit off by feeding the gases and placing the flame of a Bunsen burner on the reactor in the proximity of the catalyst. Once the catalyst is lit off, the Bunsen burner is removed and an inch thick piece of Isofrax insulation is placed around the reactor to prevent radial heat losses. The amount of insulation remained constant to avoid changes in heat losses that affect the temperature of the reactor.

Once the reactor has reached steady state, product gases are sampled with a gas tight syringe. The syringe contents are injected into an Agilent 6890 gas chromatograph (GC). The GC uses an HP-PLOT Q column to separate carbon dioxide from the other gases and a HP-PLOT 5A column is used to separate nitrogen, oxygen, methane and carbon monoxide. The gases are detected by a thermal conductivity detector using helium as the carrier gas. Since hydrogen and water are not measured in the GC, water concentration is obtained by closing the atomic oxygen balance and hydrogen is then found by closing the atomic hydrogen balance. The carbon balance is calculated and closes to within $\pm 5\%$. Each data point shown in the figures is an average over three experimental runs.

2.2. Catalyst preparation

The catalyst metals are supported on 80 ppi α -alumina foam (tortuous) monoliths that are 17 mm in diameter and 5 mm in

axial length. The monoliths are first washcoated with γ -alumina by pipeting an alumina slurry on the monolith and drying overnight. Washcoat loadings range between 2.3% and 8.7% by weight of the blank monolith. The washcoat layer adds surface area and decreases the pore diameter. The metals are deposited using the incipient wetness technique by pipeting the appropriate salt solution (hydrogen hexachloroplatinate, nickel nitrate hexahydrate, manganese (II) nitrate, chromium (III) nitrate nonahydrate and copper (II) nitrate hemipentahydrate) directly on the foam support. The catalysts are then dried overnight and calcined in air at 750 °C for 6–8 h. During the calcination of the monolith, the volatile part of the metal salt is volatilized and the metal oxide is formed. The metal loadings on the catalysts ranged between 2.2% and 6.7% metal oxide by weight of the washcoated monolith.

2.3. Reactor performance

The catalyst performance is based on the conversion of reactants and selectivities to desired products. The conversion of species i (X_i) is calculated as the ratio of the reactant consumed to that fed:

$$X_i = \frac{F_{i,\text{in}} - F_{i,\text{out}}}{F_{i,\text{in}}}$$

where $F_{i,\text{in}}$ is the flow rate of species i into the reactor and $F_{i,\text{out}}$ is the flow of species i leaving the reactor, both corrected to standard conditions (25 °C, 1 atm).

The selectivity of atom i to form species j ($S_{i,j}$) is given as:

$$S_{i,j} = \frac{v_{i,j} F_{i,\text{out}}}{\sum_k v_{i,k} F_{k,\text{out}}}$$

where $v_{i,j}$ is the stoichiometric amount of atom i in species j . The denominator is summed over all species, k . The yield of a product is the conversion multiplied by the product selectivity.

In several experiments, the effects of varying the gas hourly space velocity were investigated. The gas hourly space velocity is defined as:

$$\text{GHSV} = \frac{F_{i,\text{total}}}{\varepsilon V_{\text{monolith}}}$$

where $F_{i,\text{total}}$ is the total volumetric flow rate entering the reactor at standard temperature and pressure, ε is the monolith void fraction and V_{monolith} is the volume of the monolith.

3. Results

3.1. Feed stoichiometry

Fig. 2 shows the behavior of the (a) back face temperature, (b) methane conversion, (c) hydrogen selectivity and (d) carbon monoxide selectivity over a wide range of methane to oxygen (C/O) feed ratios. The gas hourly space velocity was maintained at 216,000 h⁻¹.

The back face temperatures of all four catalysts are similar over the entire range of C/O feed ratios. For a C/O ratio of 1.7, the temperatures range from 720 to 740 °C. As the C/O ratio

increases, the temperature decreases continuously. All four back face temperatures range from 655 to 695 °C at a C/O ratio of 2.1.

The platinum combustion catalyst obtains the highest methane conversion over the entire range of feed ratios. The metal oxide combustion catalysts show a continuous decrease in methane conversion from 89% to 73% as the feed ratio increases. The platinum catalyst obtains a methane conversion of 93% at the lowest feed ratio to 87% at the highest feed ratio.

As the feed ratio increases, the metal oxide catalysts experience a slight increase in hydrogen selectivity from 94% to 96%, whereas the platinum catalyst exhibits a range of 90–92%. The hydrogen concentration is obtained by a material balance, so it has a larger uncertainty.

All catalysts show a constant carbon monoxide selectivity over the entire range of feed ratios. The metal oxides obtain a selectivity of 86% and the platinum catalyst obtains a selectivity of 89%.

3.2. Gas hourly space velocity

Fig. 3 shows the effect of GHSV on the (a) back face temperature, (b) methane conversion, (c) hydrogen selectivity and (d) carbon monoxide selectivity. The C/O ratio in the feed was maintained at 1.7.

All catalysts show a temperature rise as the GHSV increases. The metal oxide catalysts experienced smaller temperature rises of 30 °C from on average 710 to 740 °C. The platinum catalyst exhibited a larger temperature rise of 70 °C from 670 to 740 °C.

The platinum catalyst showed the highest methane conversion starting at 88% and rising to 94% before decreasing back to 91%, as the GHSV increased. The chromium catalyst started at 86% rose to 89% and fell back to 86% as the GHSV increased. The manganese and copper catalysts showed a constant increase from 85% to 91% as the GHSV increased. The manganese and copper catalysts did not show a maximum as the GHSV increased.

As the GHSV increases, the metal oxide catalysts exhibit an increase in hydrogen selectivity, whereas the platinum catalyst shows a slight decrease or flat profile. All catalysts achieve similar hydrogen selectivity at low GHSVs, but the metal oxides obtain higher selectivities than platinum at higher GHSVs.

All catalysts show a slight increase in carbon monoxide selectivity. At the highest GHSV, the platinum catalyst achieves a slightly higher selectivity of 88% compared to 86% for the metal oxide catalysts.

3.3. Catalyst degradation

Fig. 4 shows the back face temperature, reactant conversions and selected product selectivities for (a) a Cu/Ni catalyst, (b) a Cr/Ni catalyst and (c) a Mn/Ni catalyst. The experiments were carried out for 10 h at a GHSV of 216,000 h⁻¹ and a C/O feed ratio of 1.7.

The copper catalyst shows constant oxygen conversion and carbon monoxide selectivity over the entire 10 h period. The catalyst does show an increasing hydrogen selectivity and methane conversion as the experiment progresses. The catalyst also shows

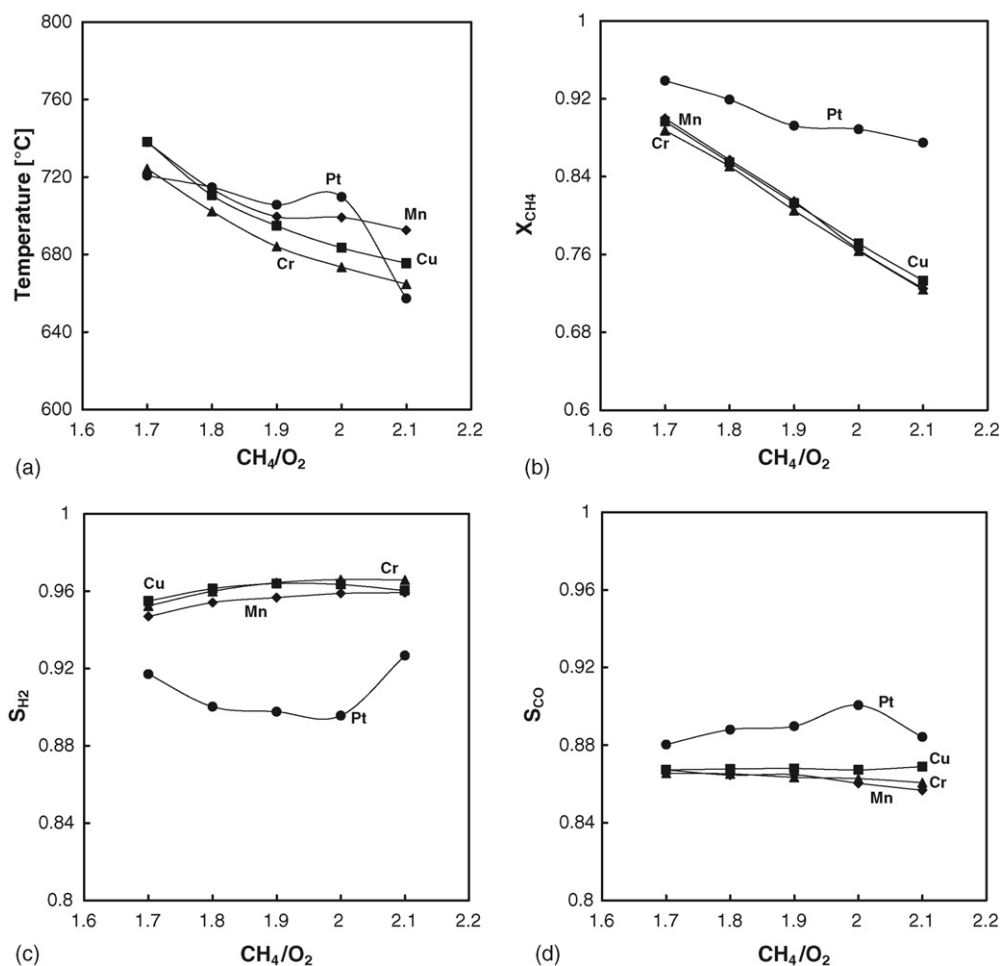


Fig. 2. Back face temperature (a), methane conversion (b), hydrogen selectivity (c) and carbon monoxide selectivity (d) for the catalytic partial oxidation of methane performed in air over manganese oxides (◆), copper oxides (■), chromium oxides (▲) and platinum (●) for varying methane to oxygen feed ratios at a GHSV of $216,000\text{ h}^{-1}$. Each data point is averaged over three different experiments. Lines are added to aid the visual presentation of the plot.

a decreasing temperature as the reaction progresses. All three parameters take nearly the full 10 h to reach steady state.

The chromium catalyst experiences similar behavior to that of the copper catalyst. Oxygen conversion and carbon monoxide selectivity are constant during the experiment. However, the methane conversion and hydrogen selectivity increase over time whereas the temperature decreases over time. These three parameters approach steady state after 10 h, but still seem to be experiencing some change, especially in the temperature.

The manganese catalyst achieves flat profiles for all parameters investigated. There is no significant change in any of the parameters over the entire 10 h experiment.

4. Discussion

4.1. Metal oxides versus platinum

Over a wide range of feed ratios and GHSVs the metal oxide catalysts achieved hydrogen yields as high or nearly as high as the platinum catalyst. For experiments in which the methane to oxygen feed ratio varied, the metal oxide catalysts showed similar temperature and carbon monoxide selectivity behavior over

the entire range. The metal oxides did exhibit a selectivity to hydrogen that averaged between 4% and 6% higher than platinum. However, the hydrogen selectivities are calculated from material balances, which add a significant amount of uncertainty to the measurement. Given this uncertainty it is not conclusive that the metal oxide catalysts give a significantly higher selectivity than platinum. In the case of methane conversion, the platinum exceeds the metal oxides by 4% at the smaller ratio and up to 16% at the higher feed ratio. Since methane concentration is measured directly it is safe to say that platinum obtains significantly better methane conversions than the metal oxide catalysts. However, at the lower ratio, which gives the highest conversion, metal oxides achieve comparable performance to the platinum catalyst.

For experiments with varying GHSV, the metal oxides and platinum catalysts again showed similar patterns in back face temperature and carbon monoxide selectivity. The metal oxides appear to obtain a higher hydrogen selectivity than platinum at larger GHSVs, but again due to uncertainty in the hydrogen selectivity measurement, it is not possible to say that any catalyst is significantly better than any other. For methane conversion, the platinum catalyst again is superior to the metal

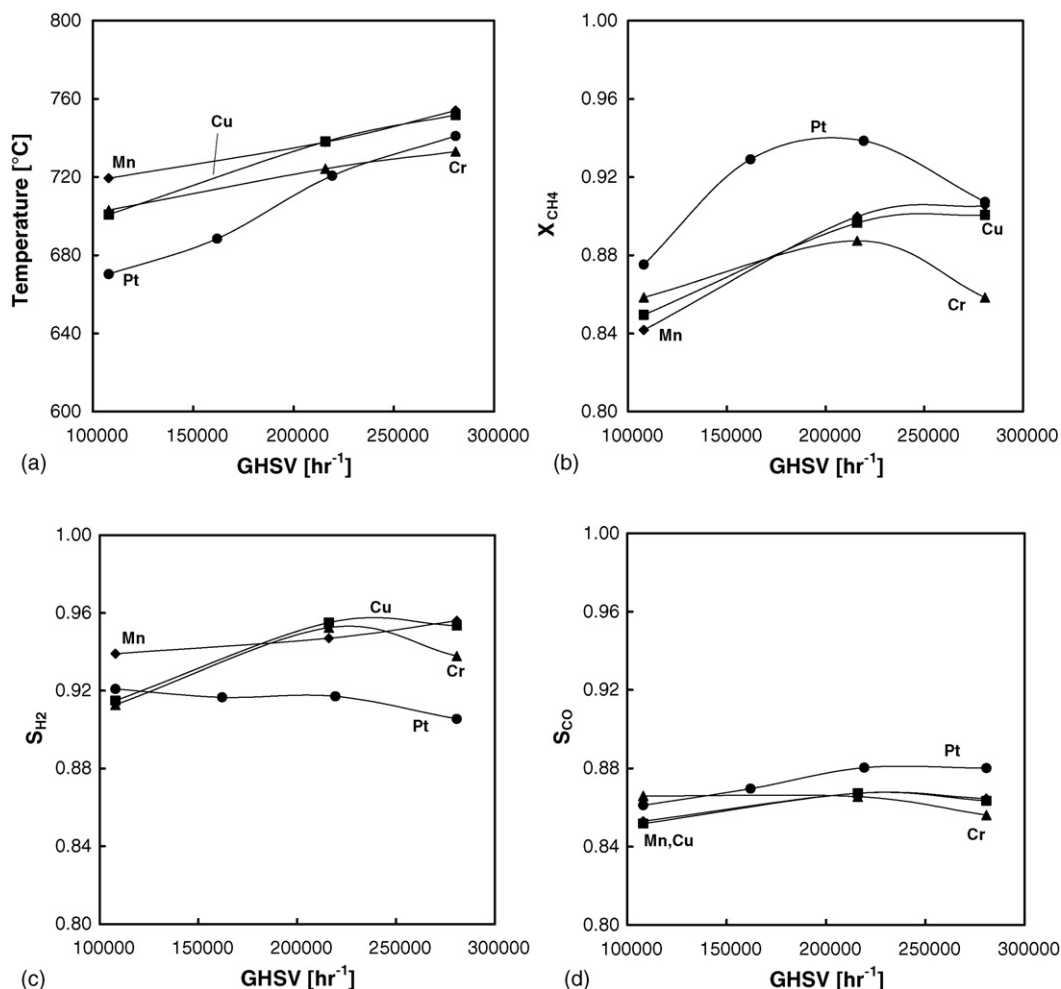


Fig. 3. Back face temperature (a), methane conversion (b), hydrogen selectivity (c) and carbon monoxide selectivity (d) for the catalytic partial oxidation of methane performed in air over manganese oxides (◆), copper oxides (■), chromium oxides (▲) and platinum (●) for varying GHSVs at a methane to oxygen ratio of 1.7. Each data point is averaged over three different experiments. Lines are added to aid the visual presentation of the plot.

oxides. Of the metal oxides, only chromium showed a maximum in methane conversion similar to the platinum catalyst. It is not yet understood why chromium experiences this peak, while manganese and copper do not. The peak is probably due to the transition from a kinetically limited regime to a mass transfer limited regime. As the GHSV increases, the heat transfer rate is increased, but the residence time for mass transfer from the bulk to the catalyst wall is decreased. At the highest GHSV, the manganese and copper catalysts achieve the same conversion as platinum with chromium being 4% lower than the others.

All three metal oxide catalysts gave stable performance over the entire 10 h period as the platinum catalyst does. The major difference is that copper and chromium did not reach a steady state as fast as the manganese and platinum catalysts. This is a subject of further research.

It is important to note that the metal oxides compare favorably to the platinum catalyst at low C/O feed ratios and high GHSVs. Both of these conditions lead to the maximum hydrogen yield of 85%. Platinum is better than metal oxides over a wide range of operating conditions, but it is not significantly better at the operating conditions, which lead to maximum hydrogen yield.

4.2. Catalyst light-off

One major difference between metal oxides and platinum catalysts is the light-off temperature. The metal oxide catalysts require a much higher temperature to light-off. For platinum catalysts, light-off occurs when the back face temperature reaches ~200 °C. However, for the metal oxides back face temperatures at light-off were 440 °C for chromium, 440 °C for manganese and 420 °C for copper. To obtain a large enough heat flux, two Bunsen burners were placed over the reactor during start-up for the metal oxide catalysts. In many cases, it was also necessary to operate at a methane to oxygen ratio of 1.2 or lower and a lower flow rate to achieve light-off. For platinum and other noble metals, one Bunsen burner was sufficient to easily light-off the catalyst at a C/O ratio of 2 and a higher flow rate.

4.3. Catalyst degradation

The catalyst degradation experiments show that over a 10 h experiment the metal oxide catalysts do not experience a drop in activity. However, the catalysts do experience some changes.

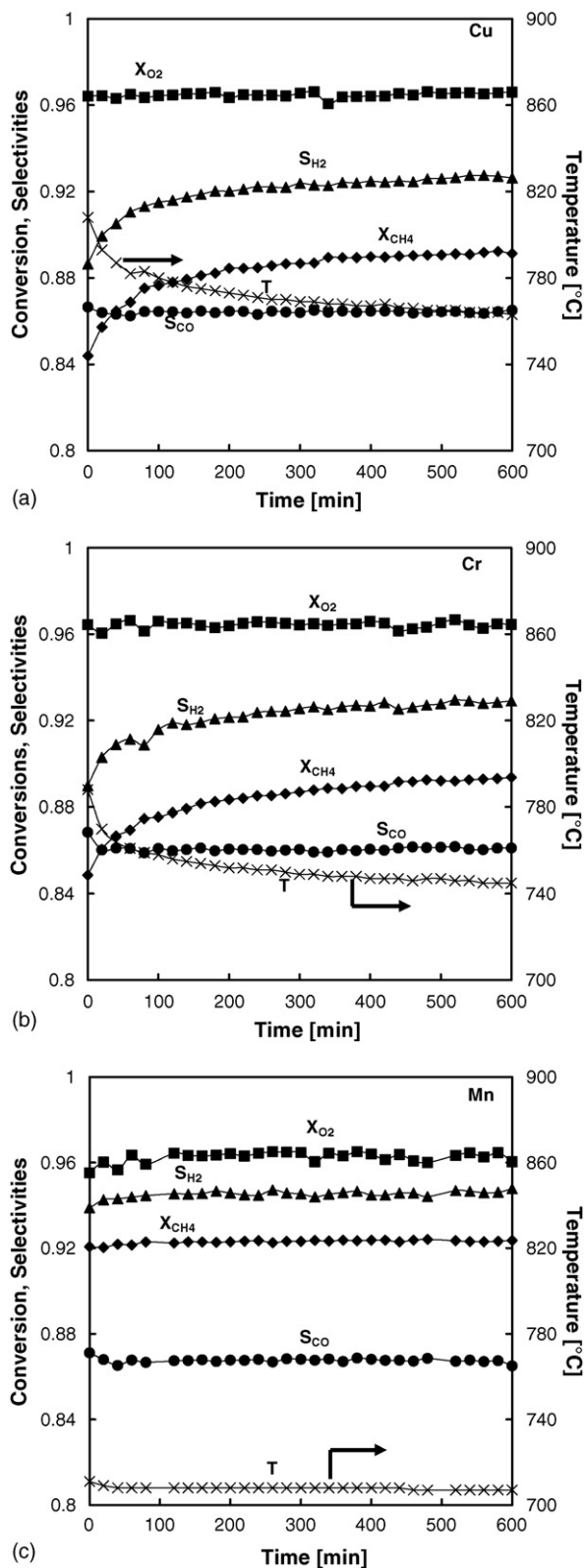


Fig. 4. Feed conversions (oxygen, ■ and methane, ◆), product selectivities (hydrogen, ▲ and carbon monoxide, ●) and catalyst back face temperatures (x, secondary axis) for copper oxides (a), chromium oxides (b) and manganese oxides (c) for a 10 h experiment.

The manganese catalyst changes from black, before use, to a dark orange. This can be explained by a reduction of the manganese from MnO_2 , which is black, to Mn_2O_3 , which is red/brown and possibly Mn_3O_4 . This is supported by a study using thermogravimetry and evolved gas analysis that found that MnO_2 is reduced to Mn_2O_3 and then Mn_3O_4 under 1000°C in the presence of oxygen and at lower temperature in nitrogen [24].

The chromium catalyst did not show a visible change in color. The chromium oxides are similar to each other in color, so a change in oxidation state may not be observable through visual inspection.

The copper catalyst was black at the beginning of the experiments. After the experiments, it is black on the upstream side and red on the downstream. Again, the upstream section probably stayed as CuO and the downstream section was reduced to Cu_2O or Cu , which are both reddish. This is supported by a previous investigation that found that at temperatures up to 1000°C , copper is in the form of CuO with oxygen present and Cu_2O or Cu when oxygen is not present [25].

The change in the manganese catalyst does not manifest as a change in catalyst activity as the reactant conversions, product selectivities and temperature do not change over time. It is likely that either both oxidation states are equally active or the transition from MnO_2 to Mn_2O_3 takes place in minutes. In the case of chromium and copper, both show a gradual change in the catalyst activity over time. It may take more time for the change in oxidation states of these metals and each state probably has a different activity. Surface analysis through characterization and spectroscopy are a subject of future investigation to determine what state each metal is in during operation. Again, it is important to note that in no case was the activity of the catalyst greatly decreased.

5. Conclusions

We have demonstrated that dual catalyst beds composed of a metal oxide combustion catalyst followed by a nickel reforming catalyst achieves similar yields of hydrogen to a platinum combustion catalyst followed by a nickel reforming catalyst. In fact, at operating conditions that optimize hydrogen yield, the metal oxide catalysts achieve the same yield as the platinum catalyst. The metal oxide catalysts demonstrated no signs of deactivation over a 10 h long experiment.

It was found that the catalysts undergo some physical changes during experimentation. Characterization and spectroscopic techniques will be used in a future investigation to determine how the catalyst is changing. Despite these qualitative changes in the catalyst, no degradation in catalytic activity was observed. The implications of this research on fuel reformers is that the catalyst cost for partial oxidation is now comparable to steam reforming, since the use of noble metals has been eliminated.

Acknowledgements

The authors would like to acknowledge the Natural Sciences and Engineering Research Council of Canada for

funding through their Discovery Grant program and the “Fonds québécois de recherche sur la nature et les technologies” for funding through their “Établissement de nouveaux chercheurs” program.

The authors would like to thank Dr. Karthik Venkataraman and Gregg Deluga for valuable critiques and discussions of the manuscript.

References

- [1] D.A. Hickman, L.D. Schmidt, *Science* 259 (1993) 343.
- [2] D.A. Hickman, L.D. Schmidt, *J. Catal.* 138 (1992) 167.
- [3] C.A. Leclerc, J.M. Redenius, L.D. Schmidt, *Catal. Lett.* 79 (2002) 39.
- [4] K.A. Williams, C.A. Leclerc, L.D. Schmidt, *AIChE J.* 51 (2005) 247.
- [5] A. Ashcroft, A. Cheetham, J. Foord, M. Green, C. Grey, A. Murrell, P. Vernon, *Nature* 344 (1990) 319.
- [6] D.A. Hickman, E.A. Hauptfear, L.D. Schmidt, *Catal. Lett.* 17 (1993) 223.
- [7] J.R. Salge, G.A. Deluga, L.D. Schmidt, *J. Catal.* 235 (2005) 69.
- [8] G.A. Deluga, J.R. Salge, L.D. Schmidt, X.E. Verykios, *Science* 303 (2004) 993.
- [9] E.C. Wanat, B. Suman, L.D. Schmidt, *J. Catal.* 235 (2005) 18.
- [10] R.P. O'Connor, E.J. Klein, L.D. Schmidt, *Catal. Lett.* 70 (2000) 99.
- [11] L.D. Schmidt, E.J. Klein, C.A. Leclerc, J.J. Krummenacher, K.N. West, *Chem. Eng. Sci.* 58 (2003) 1037.
- [12] J.J. Krummenacher, K.N. West, L.D. Schmidt, *J. Catal.* 215 (2003) 332.
- [13] P.M. Torniaainen, X. Chu, L.D. Schmidt, *J. Catal.* 146 (1994) 1.
- [14] G.C.M. Tong, J. Flynn, C.A. Leclerc, *Catal. Lett.* 102 (2005) 131.
- [15] J.H. Lee, D.L. Trimm, *Fuel Proc. Tech.* 42 (1995) 339.
- [16] T.V. Choudhary, S. Banerjee, V.R. Choudhary, *Appl. Catal. A* 234 (2002) 1.
- [17] M.I. Zaki, M.A. Hasan, L. Pasupulety, N.E. Fouad, H. Knözinger, *New J. Chem.* 23 (1999) 1197.
- [18] X. Wang, Y. Xie, *React. Kinet. Catal. Lett.* 70 (2000) 43.
- [19] X. Wang, Y. Xie, *React. Kinet. Catal. Lett.* 71 (2000) 121.
- [20] M.C. Marion, E. Garbowski, M. Primet, *J. Chem. Soc. Faraday Trans.* 86 (1990) 3027.
- [21] P. Artizzu, E. Garbowski, M. Primet, Y. Brulle, J. Saint-Just, *Catal. Today* 47 (1999) 83.
- [22] R.B. Anderson, K.C. Stein, J.J. Feenan, L.J.E. Hofer, *Ind. Eng. Chem. Res.* 53 (1961) 809.
- [23] U.S. Geological Survey, *Mineral Commodities Studies*, U.S. Dept. of the Interior, 2005.
- [24] P.K. Gallagher, F. Schrey, B. Prescott, *Thermochim. Acta* 2 (1971) 405.
- [25] J.H. Kim, V.I. Babushok, T.A. Germer, G.W. Mulholland, S.H. Ehrman, *J. Mater. Res.* 18 (2003) 1614.